Comparative study of WS_2 and Co(Ni)/WS_2 HDS catalysts prepared by *ex situ*/*in situ* activation of ammonium thiotungstate

J. Espino[a,b], L. Alvarez[a,b], C. Ornelas[a], J.L. Rico[b], S. Fuentes[c], G. Berhault,[d] and G. Alonso[a,*]

[a]*Departamento de Catálisis, Centro de Investigación en Materiales Avanzados, Chihuahua, C.P. 31109, Chihuahua, México*
[b]*Facultad de Ingeniería Química e Instituto de Investigaciones Metalúrgicas, UMSNH, Laboratorio de Catálisis, Apartado postal 52J, C.P. 58000, Morelia, Mich., México*
[c]*Departamento de Catálisis, Centro de Ciencias de la Materia Condensada (CCMC)-UNAM, Apartado postal 2681, 22830, Ensenada, B.C., México*
[d]*Laboratoire de Catalyse en Chimie Organique—UMR 6503 CNRS, Université de Poitiers, 40 Avenue du Recteur Pineau, 86022 Poitiers cedex, France*

Received ???; accepted 27 June 2003

A comparative study of the syntheses of unsupported WS_2 and M/WS_2 (M = Co, Ni) catalysts by *ex situ*/*in situ* decomposition of ammonium thiotungstate (ATT) is herein reported. *Ex situ* activation was performed under a H_2S (15% volume)/H_2 flow, whereas *in situ* activation consists in the direct decomposition of ATT or Co(Ni)/ATT precursors in the presence of a hydrocarbon solvent during the hydrodesulfurization (HDS) of dibenzothiophene (DBT). Precursors were characterized by thermogravimetric analysis and final catalysts by X-ray diffraction (XRD), scanning electron microscopy (SEM) and specific surface area (BET). Catalysts activated using the *in situ* mode of activation present higher specific surface areas with the noticeable exception of the Ni/ATT precursor. Activity measurements showed that the *in situ* activated WS_2 and Ni/WS_2 catalysts exhibit higher activity than the *ex situ* activated catalysts.

KEY WORDS: *Ex situ*/*in situ* activation; unsupported; promotion; hydrodesulfurization; WS_2.

1. Introduction

Studies on more efficient hydrotreating catalysts are nowadays stimulated by the increasingly drastic environmental regulations on sulfur, nitrogen and aromatic contents of vehicle transportation fuels and by the decreasing availability of high quality crude oil. Hydroprocessing heavy feedstock presenting high content of impurities is therefore more and more necessary [1,2]. Owing to their exceptional resistance to poisons, transition metal sulfides, mainly molybdenum and tungsten disulfide, promoted with cobalt or nickel, are widely used to remove heteroelements [3–5]. Alumina is generally used as a support because of its high superficial area and its strong interaction with MoS_2, which allows good dispersion and stabilization of the active phase [3]. Hydrodesulfurization (HDS) catalysts can be prepared by several methods, including comaceration [6] and homogeneous sulfide precipitation [7]. Recently, unsupported molybdenum and tungsten sulfide catalysts with high superficial areas have been synthesized using thiosalts as precursors [8–12]. Surface areas and catalytic properties depend strongly upon the atmosphere as well as the experimental conditions used during the activation process. For instance, large variations of surface areas have been reported for MoS_2 and WS_2 catalysts, ranging from few to several hundred square meters per gram depending on the decomposition conditions [13,14]. In this respect, *ex situ* activation, i.e., activation under a H_2/H_2S gas mixture, leads to catalytic systems with a very low surface area [15] while *in situ* activation, i.e., direct decomposition of the precursor under HDS conditions led to high surface areas [16]. Moreover, cobalt-promoted unsupported catalysts prepared from the decomposition of thiosalts have shown higher catalytic activities than promoted catalysts obtained by other methods of preparation [17,18]. Thiosalt precursors were also used successfully for alumina-supported catalytic systems. Indeed, some supported nickel-promoted tungsten catalysts formed from oxy- and thiosalts with fluorine as additive have been prepared and characterized by Prins and coworkers [19–22]. These authors showed that when ammonium thiotungstate is used as precursor, fully sulfided catalysts with a high hydrodenitrogenation activity are obtained. They also demonstrated that the incorporation of nickel increases the stacking height of small WS_2 crystallites. However, even if unsupported molybdenum sulfide catalysts have been often used as model catalysts for hydrotreating reactions, their high volumetric activities tend to be more and more attractive for commercial applications. Actually, a new quasi-unsupported catalyst called nebula with a very high activity is commercially available [23].

* To whom correspondence should be addressed.
E-mail: gabriel.alonso@cimav.edu.mx

1011-372X/03/0900–0071/0

The purpose of this work was then to study the influence of the promoter (Co or Ni) and activation methods (*in situ* and *ex situ* modes) on the activity for the hydrodesulfurization of dibenzothiophene (DBT) of catalysts prepared from ammonium thiotungstate (ATT).

2. Experimental

2.1. Preparation of samples

Ammonium metatungstate was dissolved in 200 mL of distilled water and 20 mL of ammonium hydroxide (ACS reagent) was added to this solution. The ammoniacal solution was then heated at 333 K and H_2S was bubbled through the solution for 6 h. The solution was then cooled to room temperature and left to stand overnight. Orange needle-like ATT crystals were then obtained [14,24]. For promoted catalysts, the required amount of $Co(NO_3)_2 \cdot 6\ H_2O$ or $Ni(NO_3)_2 \cdot 6\ H_2O$ was added to give an atomic ratio of $R = Co/(Co + W) = 0.3$ and $R = Ni/(Ni + W) = 0.5$ respectively. Nickel or cobalt nitrate was first dissolved in the minimum amount of water and dripped to ATT crystals, a soft paste was formed, which was then dried at 393 K for 2 h. The precursors were activated by *ex situ* or *in situ* methods of activation. The *ex situ* catalysts were activated under a H_2/H_2S gas flow (15% H_2S v/v) by heating the precursor at 4 K/min from room temperature to 673 K for 4 h prior to the catalytic test. *In situ* activated catalysts were formed by thermal decomposition of precursors in the liquid phase during the HDS of DBT (see following section for experimental conditions). The *ex situ* activated catalysts were named $WS_{2\ ex\ situ}$, $Ni/WS_{2\ ex\ situ}$, $Co/WS_{2\ ex\ situ}$ and the *in situ* activated ones, $ATT_{in\ situ}$, $Ni/ATT_{in\ situ}$, and $Co/ATT_{in\ situ}$.

2.2. Catalytic activity and selectivity

The HDS of DBT was carried out in a Parr Model 4520 high-pressure batch reactor. The *ex situ* activated catalyst (1.0 g) or, for the *in situ* mode of activation, the appropriate amount of precursor to yield 1 g of WS_2 or M/WS_2 was placed in the reactor. The reactant mixture (5% volume of DBT in decalin) was then added and the autoclave was then pressurized with hydrogen to 3.1 MPa and heated up to 623 K at 10 K/min. Once at 623 K, the reaction was followed for 5 h by analyzing samples using a Perkin Elmer AutoSystem XL gas chromatography equipped with an OV-17 packed column.

The main reaction products for the HDS of DBT are biphenyl (BiPh) formed by direct C–S bond cleavage of DBT (the so-called direct desulfurization pathway, DDS), and phenylcyclohexane (PhCH) formed by an initial hydrogenation of one of the aromatic rings of DBT followed by C–S bond rupture (the hydrogenating pathway, HYD). The selectivity for the main reaction products was determined for WS_2 and Co(Ni)-promoted WS_2 catalysts. The HYD/DDS selectivity ratio is based on the product concentration ratio (PhCH/BiPh). It should be noted that an intermediate primary hydrogenated product, tetrahydrodibenzothiophene (THDBT) is formed along the HYD pathway. Its concentration stays low and could be neglected when calculating the HYD/DDS ratio. Moreover, this compound is not an HDS product since it still contains sulfur. The mean standard deviation for catalytic measurements was about 2.5%. After the DBT reaction, the catalysts were separated from the reaction mixture by filtration, washed with isopropanol to remove residual hydrocarbons and dried at room temperature before elemental analysis.

2.3. Catalyst characterization

The differential thermal analysis (DTA) and thermogravimetric analysis (TGA) of the thiosalt precursors were obtained simultaneously on a TA instruments SDT 2960 DTA-TGA equipment, heating the sample from 298–823 K at 4 K/min under dry nitrogen flow. *Ex situ* activated catalysts were characterized before and after the HDS reaction while characterization of *in situ* activated catalysts was performed after the HDS catalytic test. Specific surface areas were measured with a Quantachrome Nova 1000 series by nitrogen adsorption at 77 K using the BET method. Samples were degassed under vacuum at 523 K before nitrogen adsorption. Catalyst morphology was studied using a JEOL JSM-58000LV scanning electron microscope analyzing several fields at different magnifications to aid in the recognition of prevalent features. The surface composition of catalysts was determined by Energy Dispersive Spectroscopy using the EDAX CDU Leap Detector method. The relative atomic ratios for tungsten, sulfur and promoters at the surface were calculated for all samples after the HDS catalytic test. X-ray Diffraction (XRD) studies were performed using a Phillips X Pert MPD diffractometer equipped with a curved graphite monochromator using Cu Kα radiation ($\lambda = 1.54056$ Å) operating at 43 kV and 30 mA.

3. Results

3.1. Thermal analysis

Thermogravimetric and differential thermal analyses were used to characterize the thermal decomposition of ATT, Ni/ATT and Co/ATT precursors. Transition temperatures and thermal decomposition curves are reported in table 1 and figure 1 respectively. As shown in

Table 1
Thermogravimetric analysis of ATT, NiATT and CoATT precursors decomposed under nitrogen atmosphere

	ATT	Ni/ATT	Co/ATT
T_{-1} (K)	–	350	350
Δw_{-1}, wt% (exp)	–	2	2
Assuming water			
T_1 (K)	465	350	350
T_2 (K)	550	520	490
Δw_1, wt% (exp)	19.2	33	8.0
Δw_1, wt% (theor)	19.6	36	8.9
assuming loss	$2NH_3+H_2S$	$2NH_3+2HNO_3+S^0$	$2S^0$
T_3 (K)	680	–	550
Δw_2, wt% (exp)	9.0	–	9.0
Δw_2, wt% (theor)	9.2	–	9.5
assuming loss	S^0		$(NH_4)_2S$
T_4 (K)	–	–	650
Δw_3, wt% (exp)	–	–	13.4
Δw_3, wt% (theor)	–	–	13.4
assuming loss			$3S^0$
Residual, wt% (exp)	71.8	67	69.6
Residual, wt% (theor)	71.2	64	68.2
assuming residual as	WS_2	$NiWS_3$	$Co(WS)_2$

figure 1(a), the ATT thermogram presents two steps of decomposition with an endothermic peak at 525 K and an exothermic peak at 630 K. Ni/ATT and Co/ATT thermograms (see figures 1(b) and (c) respectively) exhibit one initial step at 350 K of about 2 wt%, which is attributed to the loss of water. In addition, the Ni/ATT thermogram shows one single step of decomposition with an exothermic peak at 450 K. Interestingly, the Co/ATT thermogram is more complex with three main steps, the first step exhibiting an exothermic peak at 450 K, the second step an endothermic peak at 525 K while the third step shows once again an exothermic peak at 650 K.

3.2. Elemental analysis

S/(M + W) and M/(M + W) atomic ratios (M = Co or Ni) determined using EDS analysis are reported in table 2. For nonpromoted WS_2 catalysts prepared either *in situ* or *ex situ*, the S/W experimental ratio is always lower than the theoretical value of 2.0. The $Ni/WS_{2\ ex\ situ}$ as well as the $Co/ATT_{in\ situ}$ catalysts present S/(M + W) experimental ratios quite close to the values expected theoretically. Surprisingly, the $Ni/ATT_{in\ situ}$ and $Co/WS_{2\ ex\ situ}$ catalysts exhibit a large excess of sulfur since S/(M + W) experimental values are twice higher than the theoretical ratio. Finally, the promoter ratio, $R = M/(M + W)$, is still slightly higher than expected according to the desired values ($R = 0.3$ for cobalt and $R = 0.5$ for nickel). This result suggests that even if nickel or cobalt nitrate solutions react immediately with ATT crystals to form a soft paste.

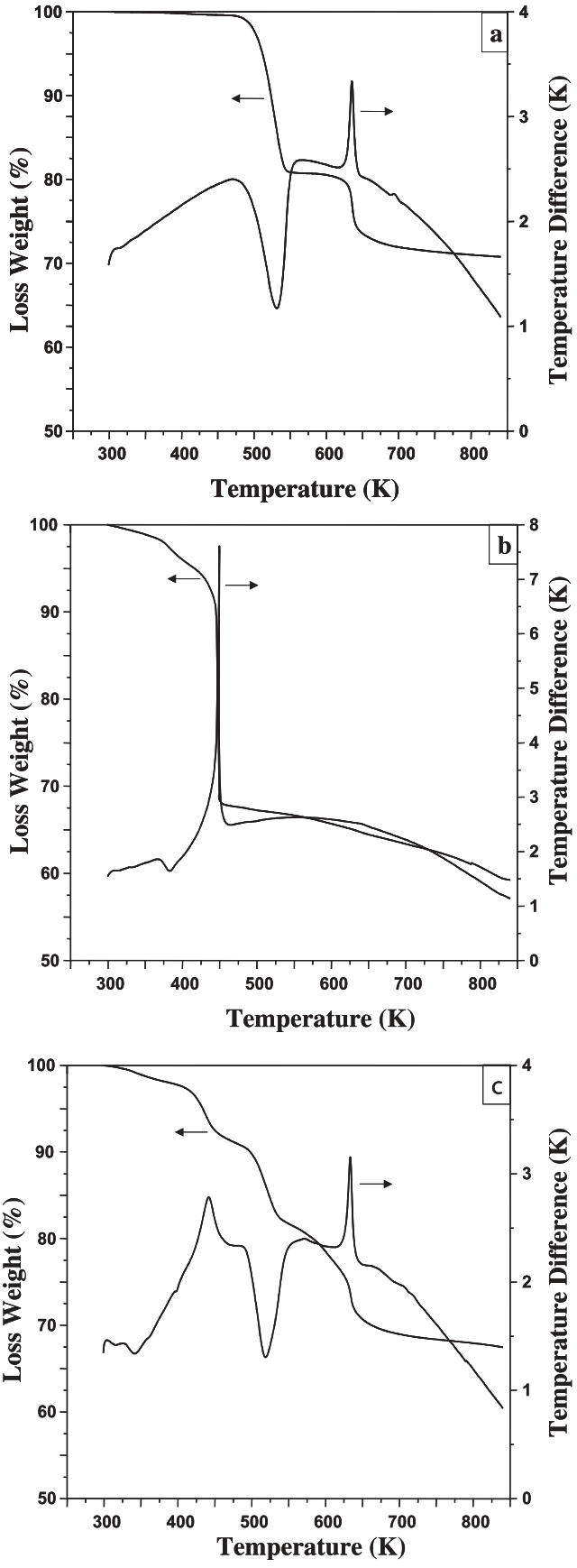

Figure 1. DTA–TGA curves of the decomposition of (a) ATT, (b) Ni/ATT, and (c) Co/ATT precursors.

Table 2
Specific surface area results and elemental analysis for nonpromoted and Co(Ni)/WS_2 catalysts prepared using *ex situ* or *in situ* modes of activation. Surface areas were measured before and after the HDS catalytic test for *ex situ* activated catalysts. S/(M + W) and M/(M + W) atomic ratios were determined after the HDS catalytic test (M = Co or Ni)

Catalyst	Specific surface areas (m^2/g)		Atomic ratio	
	Before reaction	After reaction	S/(M + W)[a]	M/(M + W)
$ATT_{in\ situ}$	–	56.6	1.5 (*2.0*)	–
$WS_{2\ ex\ situ}$	12.8	11.3	1.7 (*2.0*)	–
$Ni/ATT_{in\ situ}$	–	16.0	1.7 (*0.8*)	0.7
$Ni/WS_{2\ ex\ situ}$	17.7	18.6	0.9 (*0.9*)	0.6
$Co/ATT_{in\ situ}$	–	31.6	1.2 (*1.3*)	0.4
$Co/WS_{2\ ex\ situ}$	10.5	11.7	2.3 (*1.2*)	0.5

[a] Values in italics correspond to the theoretical S/(M + W) ratio, considering the M/(M + W) experimental ratio and Ni_3S_2, Co_9S_8 and WS_2 as the thermodynamic stable phases.

3.3. Surface area

Specific surface areas for all catalysts are reported in table 2. Surface areas for the *in situ* activated samples were measured after the HDS reaction, whereas for the *ex situ* activated catalysts surface areas were measured before and after the HDS reaction. *In situ* mode of activation generally results in higher surface areas than the *ex situ* preparation. Indeed, the nonpromoted catalyst reaches a value of 56.6 m^2/g after the *in situ* activation while the *ex situ* preparation leads to a much lower surface area (11.3 m^2/g). A similar situation is observed for the Co-containing catalysts with a surface area three times higher after the *in situ* activation. Exception is for the Ni-containing catalysts with similar surface areas for both types of activation. For the *in situ* mode of activation, cobalt or nickel promotion leads to a decrease of surface area compared to the $ATT_{in\ situ}$ catalyst, whereas for the *ex situ* mode of activation, promotion does not involve any real variation of the final surface area. Finally, *ex situ* activated catalysts appeared quite stable during hydrodesulfurization since no loss of surface area was detected after the HDS test.

3.4. Catalytic activity and selectivity

Table 3 reports activity and selectivity results for the HDS of DBT. The *in situ* mode of activation leads to better active catalysts than the *ex situ* activation since nonpromoted and nickel-containing catalysts exhibit a 40% increase in activity when *in situ* activated compared to their *ex situ* activated counterparts. For cobalt-containing catalysts, $Co/ATT_{in\ situ}$ is only 20% more active than $Co/WS_{2\ ex\ situ}$. Nickel addition results in a marked increase in activity for both *in situ* or *ex situ* modes of activation revealing a synergetic effect between Ni and W. This situation differs strongly from the cobalt-containing catalysts, which present similar activity results after cobalt addition compared to nonpromoted catalysts. This result confirms previous results showing that the synergy between Co and W is an unsuccessful combination [25,26]. Moreover, both cobalt and nickel addition favors selectivity along the DDS pathway [27].

3.5. X-ray diffraction

Figures 2(a) and (b) report the XRD patterns for *ex situ* activated catalysts before and after the HDS catalytic reaction and for *in situ* activated catalysts after the catalytic test. As shown in figure 2(a), XRD patterns for *ex situ* activated catalysts before or after the HDS test present weak peaks corresponding to a very poorly crystalline structure characteristic of the tungsten disulfide phase. A noticeable exception is the XRD pattern of the $Ni/WS_{2\ ex\ situ}$ catalyst before the test. The intensity of the (002) peak at $2\Theta = 14^\circ$, characteristic of the layer stacking along the *c* direction, is quite low for all *ex situ* prepared samples. Therefore, the *ex situ* activated catalysts are probably composed of WS_2 particles with very few stacked layers [28]. It should be noted that HDS conditions can induce some morphological modifications for the *ex situ* activated catalysts.

Table 3
Initial rates constants, DBT conversion and selectivity (HYD/DDS) for *in situ* and *ex situ* activated catalysts. DBT HDS conversion was measured after 5 h onstream

Catalyst	$k*10^7$ (mol s^{-1} g cat^{-1})	DBT conversion (% mol)	HYD/DDS ratio
$ATT_{in\ situ}$	6.5	31.8	1.4
$WS_{2\ ex\ situ}$	4.7	20.0	1.4
$Ni/ATT_{in\ situ}$	13.6	59.7	0.6
$Ni/WS_{2\ ex\ situ}$	9.7	45.7	1.0
$Co/ATT_{in\ situ}$	6.5	28.4	0.5
$Co/WS_{2\ ex\ situ}$	5.5	25.5	0.6

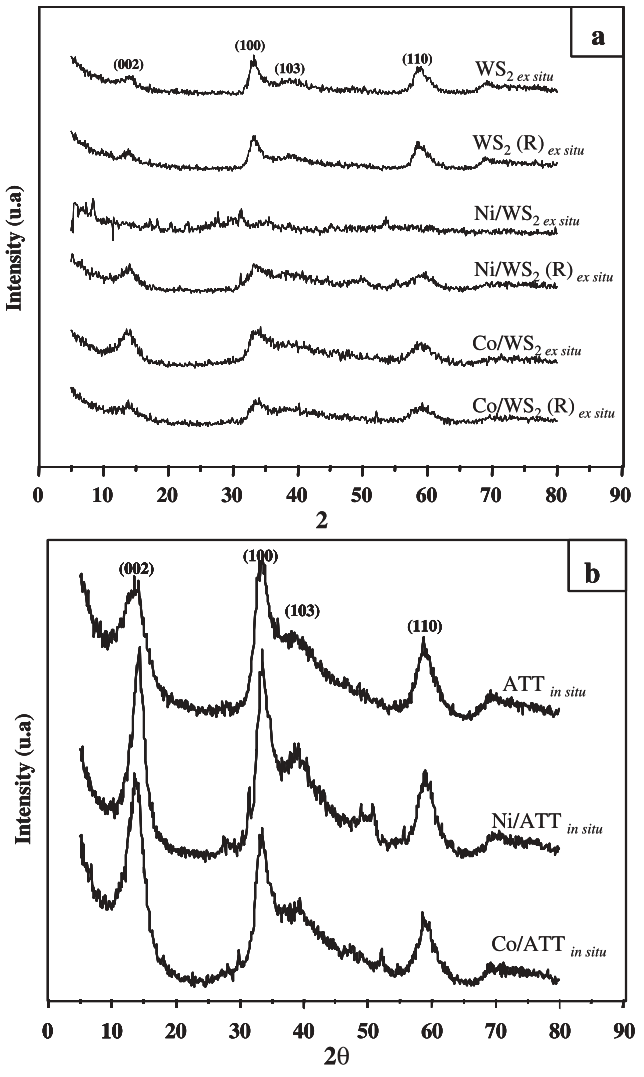

Figure 2. XRD patterns of (a) *ex situ* activated catalysts before and after (R) the HDS test, and of (b) *in situ* activated catalysts after the catalytic reaction.

While the nonpromoted $WS_{2\ ex\ situ}$ catalyst does not show any evolution of its XRD pattern before and after the catalytic reaction, the $Co/WS_{2\ ex\ situ}$ catalyst exhibits weaker XRD peaks after the HDS test. The $Ni/WS_{2\ ex\ situ}$ catalyst presents a very different comportment with no noticeable XRD peaks before the HDS test but with the appearance of peaks characteristic of the layered tungsten disulfide phase after the catalytic reaction. For *in situ* activated samples (see figure 2(b)), XRD patterns differ strongly from those obtained for *ex situ* activated catalysts. Quite strong diffraction peaks are observed with a well-defined (002) peak, particularly intense for cobalt- and nickel-containing catalysts. Consequently, *in situ* activated catalysts appear largely more crystalline than catalysts prepared using the *ex situ* mode of activation. Finally, for both cases, XRD patterns did not present peaks of Co or Ni phases, suggesting that promoter atoms are well dispersed on the active phase.

3.6. Scanning electron microscopy

Micrograph of the *ex situ* unpromoted catalyst (cf. figure 3(a)) shows a very compact shape while for the *in situ* unpromoted sample (cf. figure 3(b)), morphology of the particles appears more cracked. This observation explains the low surface area obtained for the compact $WS_{2\ ex\ situ}$ catalyst, whereas a fivefold increase in surface area is observed for the $ATT_{in\ situ}$ catalyst (cf. table 2). Comparison of the *ex situ* prepared nickel-containing catalyst, $Ni/WS_{2\ ex\ situ}$ (cf. figure 3(c)), with its *in situ* counterpart, $Ni/ATT_{in\ situ}$ (cf. figure 3(d)), does not reveal any real difference between the two samples, which is confirmed by their quite similar surface areas (cf. table 2). For the cobalt-containing catalysts, while the *ex situ* prepared sample, $Co/WS_{2\ ex\ situ}$ seems to be a relatively dense material (cf. figure 3(e)), $Co/ATT_{in\ situ}$ presents a more open morphology (cf. figure 3(f)) explaining once again the higher surface area of the *in situ* activated sample.

4. Discussion

Textural and structural properties of WS_2 catalysts obtained by *ex situ* and *in situ* decompositions of thiotungstate precursors have been reported to be comparable to those obtained for the MoS_2 catalysts prepared using similar methods of activation [14,29,30]. However, some differences exist between WS_2 and MoS_2 catalysts and have been attributed to a larger resistance to sintering and a better crystalline organization of WS_2 compared to MoS_2 [13,31].

The DTA–TGA study of the ATT precursor (cf. table 1 and figure 1(a)) shows two steps of decomposition. The first step can be attributed to the formation of ammonia, hydrogen sulfide and tungsten trisulfide, according to reaction (1) [8]:

$$(NH_4)_2WS_4 \rightarrow WS_3 + 2NH_3 + H_2S \qquad (1)$$

This reaction occurs between 465 and 550 K with an endothermic peak at 525 K. The experimental weight loss for reaction (1) was found to be 19.2% (theoretical 19.6%). Tungsten trisulfide appears to be stable in the region between 550 and 610 K but decomposes to WS_2 from 610 to 680 K with an exothermic peak at 630 K, with the simultaneous reduction of W^{6+} to W^{4+} and oxidation of S^{2-} to S^0:

$$WS_3 \rightarrow WS_2 + S^0 \qquad (2)$$

The experimental weight loss for reaction (2) was found to be 9.0% (theoretical 9.2%).

The Ni/ATT and Co/ATT bimetallic precursors decompose according to the model proposed by Pedraza *et al.* [10]. The thermal decomposition of Ni/ATT occurs

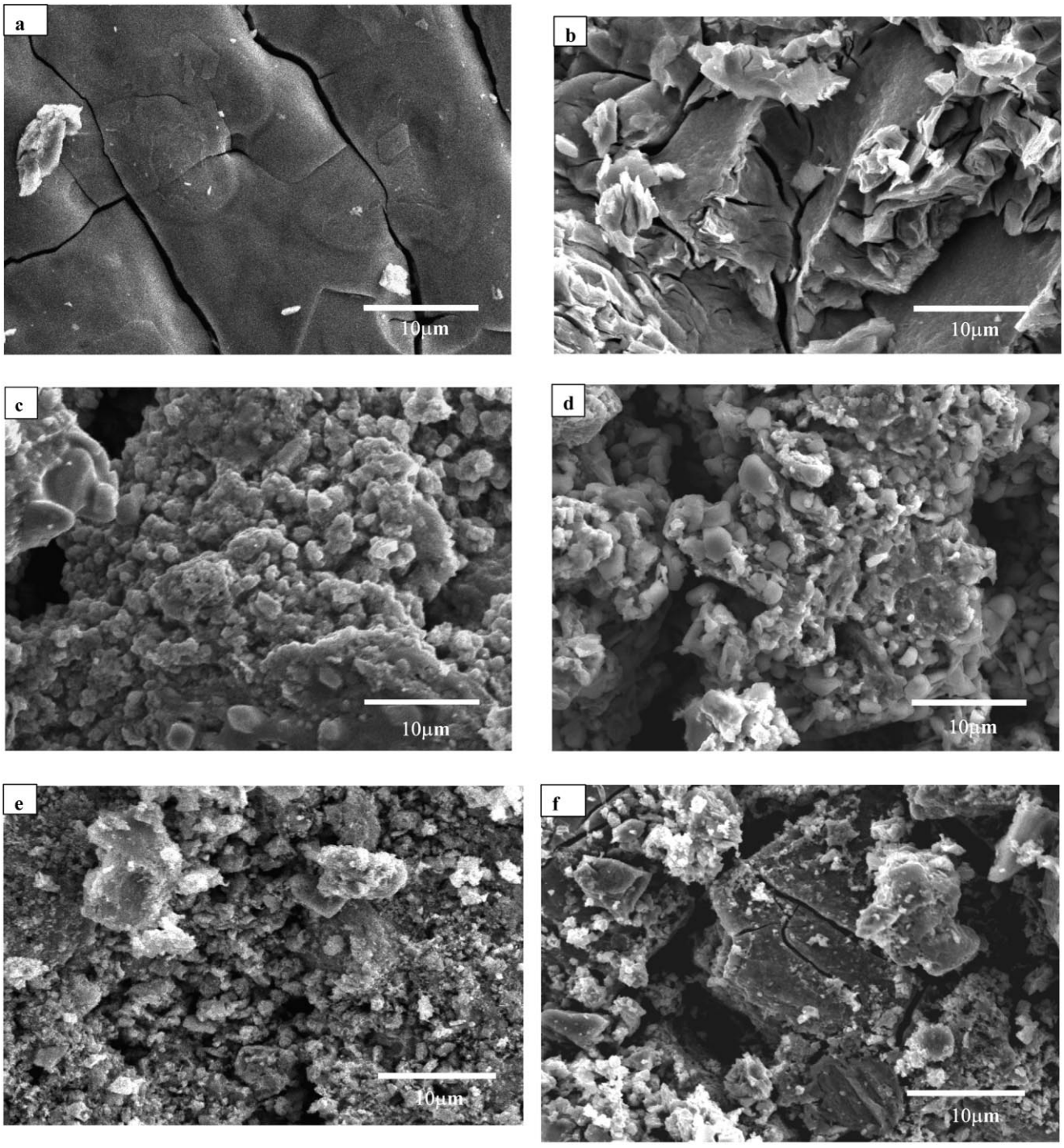

Figure 3. Scanning electron micrographs of the (a) $WS_{2\ ex\ situ}$, (b) $ATT_{in\ situ}$, (c) $Ni/WS_{2\ ex\ situ}$, (d) $Ni/ATT_{in\ situ}$, (e) $Co/WS_{2\ ex\ situ}$, and (f) $Co/ATT_{in\ situ}$ catalysts.

in a single step according to reaction (3):

$$(NH_4)_2WS_4 + Ni(NO_3)_2 \rightarrow NiWS_4[2NH_4NO_3] \rightarrow NiWS_3 + 2NH_3 + 2HNO_3 + S^0 \quad (3)$$

This step of decomposition is strongly exothermic and occurs in the 350–520 K temperature range with a weight loss of 33% (theoretical 36%). The exothermic peak appears at 450 K.

Interestingly, the decomposition of the Co/ATT precursor is quite complicated owing to the fact that

ATT and cobalt nitrate react first according to the following reaction:

$$2(NH_4)_2WS_4 + Co(NO_3)_2 \rightarrow (NH_4)_2Co(WS_4)_2[2NH_4NO_3] \quad (4)$$

When this mixture is dried at 393 K, the ammonium nitrate in excess leaves the system forming nitric acid and ammonia:

$$(NH_4)_2Co(WS_4)_2[2NH_4NO_3] \rightarrow (NH_4)_2Co(WS_4)_2 + 2HNO_3 + 2NH_3 \quad (5)$$

The as-formed precursor $(NH_4)_2Co(WS_4)_2$ shows three steps of decomposition. The first step occurs in the 350–490 K temperature range with an exothermic peak at 450 K. The weight loss is 8.0% (theoretical 8.9%) and corresponds to the elimination of 2 S^0:

$$(NH_4)_2Co(WS_4)_2 \rightarrow (NH_4)_2Co(WS_3)_2 + 2S^0 \quad (6)$$

The second step is endothermic and occurs at 525–550 K. The weight loss is 9.0% (theoretical 9.5%) and corresponds to the elimination of ammonium sulfide:

$$(NH_4)_2Co(WS_3)_2 \rightarrow Co(WS_2)_2S + (NH_4)_2S \quad (7)$$

The last step occurs at 625–650 K with an exothermic peak and a weight loss of 13.4% (theoretical 13.4%) assigned to further elimination of sulfur, according to the following equation:

$$Co(WS_2)_2S \rightarrow Co(WS)_2 + 3S^0 \quad (8)$$

As expected, the different experimental conditions used in the *in situ* or *ex situ* modes of activation strongly influence the final specific surface areas of the unsupported WS_2-based catalysts studied here. The *in situ* activation in the presence of a hydrocarbon solution leads to a strong increase in the surface area for both nonpromoted and cobalt-containing WS_2 catalysts. Interestingly, nickel-promoted WS_2 catalysts do not show any change of surface area if prepared *in situ* or *ex situ*. A possible explanation for this difference of comportment between catalysts formed from ATT (or Co/ATT) and Ni/ATT precursors could be found in their mode of decomposition as observed in the DTA–TGA study. While the decomposition of the ATT or Co/ATT precursor results mainly in a tungsten sulfide phase (potentially in close contact with Co atoms for Co/ATT), the decomposition of the Ni/ATT precursor seems to lead only to a Ni/WS_3 phase as early as 500 K. However, it should be underlined that the *in situ* or *ex situ* decomposition was performed in the presence of H_2 and not N_2 as for the DTA–TGA study. Anyway, the absence of any change in surface area for nickel-containing catalysts may be related to the formation of this tungsten trisulfide phase, which was only subsequently transformed into a WS_2-like phase. In this respect, while XRD patterns for $WS_{2\ ex\ situ}$ and $Co/WS_{2\ ex\ situ}$ before the HDS reaction reveal characteristic tungsten sulfide peaks, $Ni/WS_{2\ ex\ situ}$ before the HDS reaction does not show any detectable peak. This result is in agreement with the well-known amorphous nature of the WS_3 phase [32–35].

The *ex situ* method of preparation generally leads to a very poorly crystalline phase in contrast with *in situ* prepared samples. The gas-phase activation under H_2/H_2S results in much lower crystalline catalysts than samples decomposed in an autoclave in the presence of a hydrocarbon solution. This lower degree of crystallization might be related to a faster decomposition rate for thiosalt precursors when decomposed under H_2/H_2S or to experimental conditions for which hydrocarbons act as "softer" reducing agents than the H_2/H_2S mixture. Indeed, hydrocarbon fragments can play the role of less tough reducing agents than H_2 for the activation of hydrotreating catalysts [36,37]. Moreover, for the *ex situ* activated samples, comparison of the XRD patterns before and after the catalytic reaction reveals quite different evolution of their morphology during the HDS test. While the nonpromoted $WS_{2\ ex\ situ}$ catalyst hardly changes under hydrodesulfurization conditions, the $Co/WS_{2\ ex\ situ}$ catalyst shows a decrease in stacking height. Finally, the $Ni/WS_{2\ ex\ situ}$ catalyst presents a definite XRD pattern of a WS_2 phase after the HDS test, suggesting that the final WS_2 structure is only achieved for this catalyst if submitted to HDS conditions. However, surprisingly, these changes in morphology are not accompanied by any loss or gain in surface area. It should be noted anyway that surface areas were already quite low before the HDS test.

Unpromoted and nickel-promoted WS_2 catalysts exhibit an increase in activity for the HDS of DBT if *in situ* activated. Recent progress about the role of carbonaceous species in hydrotreating reactions could help in explaining this result [11,12,37–44]. As observed by Glasson *et al.* [38], carbonaceous species can interfere during the initial stages of the formation of the transition metal sulfide phase by blocking crystalline growth of sulfide particles. This interaction of carbonaceous species prevents the catalytic system from sintering and maintains a good dispersion of the active phase. The early interaction between the forming WS_2 catalyst and carbonaceous species is probably fulfilled for the *in situ* mode of activation since the thiosalt precursor is in close contact with a hydrocarbon solution. For the *ex situ* method of preparation, the final WS_2-like phase is already formed during the H_2/H_2S treatment before any contact with the hydrocarbon solution. Strikingly, the beneficial effect of an *in situ* mode of activation is not observed for the cobalt-containing catalysts. The DTA–TGA study of the Co/ATT precursor shows a complex decomposition path-

way leading around 625–650 K to a $Co(WS)_2$ residual stoichiometry. Such a composition would correspond to a certain degree to a sulfur deficiency, even accentuated by a reducing atmosphere instead of an inert gas like in the DTA–TGA study. This result would mean that the initial decomposition during heating at 623 K under H_2/H_2S or in an autoclave leads to a phase that does not present any synergetic effect for HDS between Co and W. Indeed, activities for the nonpromoted catalysts ($ATT_{in\ situ}$ and $WS_{2\ ex\ situ}$) are equal or close to the values measured for cobalt-containing catalysts ($Co/ATT_{in\ situ}$ and $Co/WS_{2\ ex\ situ}$). This result is not surprising since Co-W is an unsuccessful combination for HDS [25,26] as observed by Niemantsverdriet and coworkers. As revealed by these authors, sulfidation of the Co oxide precursor occurs before the more difficult sulfidation of WO_3 into WS_2, resulting in a quite low decoration of WS_2 edges by Co. This situation differs from the Co–Mo combination since Mo is easier to sulfide than W. In that case, the use of chelating agents retarding the sulfidation of the Co phase can reverse the order of sulfidation (W before Co) leading to a more efficient Co decoration of the WS_2 edges.

The relationship between specific surface areas and the HDS rate coefficients is not straightforward and indicates that a larger surface area does not necessarily imply a higher reaction-rate coefficient. This situation is common for anisotropic layered materials and this represents a major ongoing challenge in this field. Indeed, even if $Ni/ATT_{in\ situ}$ exhibits a low surface area, its HDS activity is the highest among all the studied catalysts. The nonpromoted WS_2 catalysts show the highest selectivity along the HYD pathway. However, no difference in selectivity could be detected between the *in situ* activated sample, $ATT_{in\ situ}$ and the *ex situ* one, $WS_{2\ ex\ situ}$. The Rim-edge model proposed by Daage and Chianelli [45] provides a direct relationship between change of morphology of the unsupported $MoS_2(WS_2)$ particles, i.e., change of stacking height of the layers, and selectivity modifications. ''Rim'' sites located at the extremities of the $MoS_2(WS_2)$ slab are active for hydrogenation and hydrogenolysis (C–S bond breaking) and ''edge'' sites located on internal stacked layers are active only for hydrogenolysis. Application of this model is not easy here because of the weak intensity of the XRD patterns for the *ex situ* activated samples. Nevertheless, compared to the $WS_{2\ ex\ situ}$ catalyst, the increase in activity observed for the *in situ* activated sample, $ATT_{in\ situ}$, without concomitant change in selectivity would mean, according to the Rim-edge model, that WS_2 particles are smaller along the basal direction after an *in situ* activation while the stacking height would be similar for both nonpromoted samples. This fact might appear contradictory to the higher degree of crystallization observed for *in situ* prepared samples and further characterization is needed to clarify this point. For nickel-promoted catalysts, selectivity along the DDS pathway is enhanced particularly for the $Ni/ATT_{in\ situ}$ catalyst. This result is in agreement with previous results [46–49] showing that nickel promotion favors the DDS pathway probably thanks to an increase of the basicity of sulfur atoms shared between Ni and Mo atoms [47]. Indeed, assuming an E_2-elimination mechanism for C–S bond rupture, an increase of basicity would favor the initial attack of β H atoms of the DBT molecule (scheme 1) [46]. The cobalt case differs strongly from the Ni-containing catalytic system since, as observed previously, no increase in activity is detected after the cobalt addition. However, surprisingly, the selectivity along the DDS pathway is also

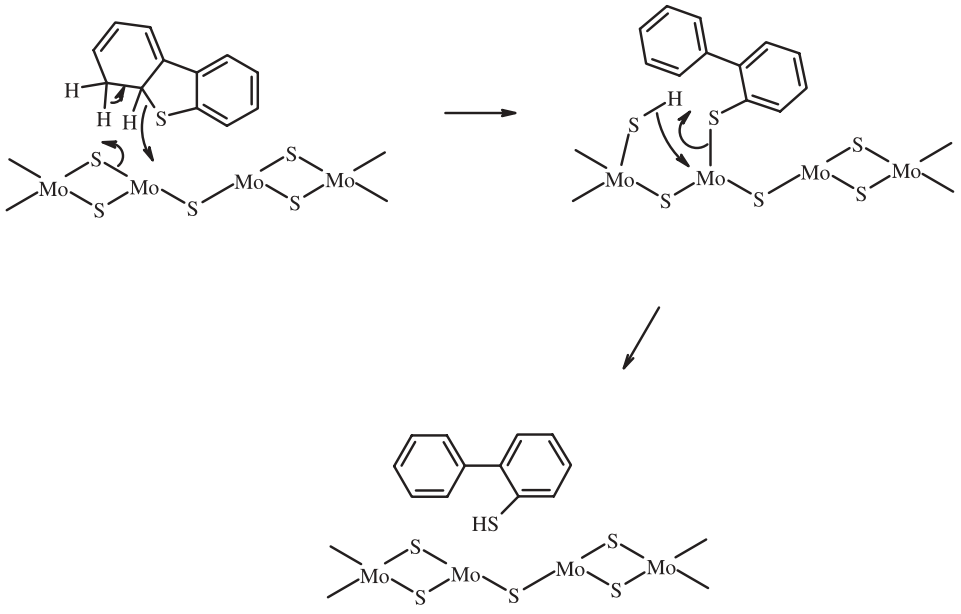

Scheme 1. Mechanism of the C–S bond cleavage in the DDS pathway for the HDS of DBT [46].

favored. This result might mean that the lack of synergy for the Co-W catalysts does not necessarily imply the absence of interaction between Co and W atoms. Indeed, Co atoms seem to influence the selectivity in the same way as Co-Mo, Ni-Mo and Ni-W catalysts. This point is quite interesting and should be further studied. The nickel or cobalt addition results in a stronger XRD (002) peak, i.e., more stacked slabs. This result is in agreement with previous results showing that promoter addition should favor the more active HDS multistacked type II-Co(Ni)MoS structures for unsupported catalysts or for catalysts dispersed on supports interacting weakly with the active phase [50,51]. Moreover, as reported by Chianelli *et al.* [52], Co decoration at the edges of MoS_2 slabs can induce an increase of the stacking height. Nevertheless, it should be noted that the Rim-edge model was never extended to promoted catalytic systems and should not be used in a strict point of view even if this increase of the stacking due to promoter atoms would favor the DDS pathway.

5. Conclusions

Depending upon the way of decomposing the precursors, significant textural and catalytic properties were observed after *in situ* (hydrocarbon solution, HDS conditions) or *ex situ* (H_2/H_2S) modes of activation. Except for Ni-containing catalysts, the *in situ* method of preparation results in catalytic systems with higher specific surface areas than their *ex situ* counterparts. Contrary to ATT and Co/ATT precursors decomposed into WS_2-type catalysts, the DTA–TGA study of the Ni/ATT precursor suggests a quite different decomposition mode with formation of a WS_3-like phase, which is only subsequently transformed into a WS_2-based catalyst under HDS conditions. XRD results showed that higher crystalline samples are obtained if catalysts are prepared using the *in situ* activation. The hydrocarbon solution acting as a "softer" reducing agent during the decomposition of the thiosalt precursors could be responsible for these differences. Activities for the HDS of DBT are still higher if catalysts are activated using the *in situ* method of preparation. The *in situ* treated nickel-promoted tungsten sulfide catalyst shows the highest reaction-rate coefficient. The absence of a synergetic effect between cobalt and tungsten confirms the difficulty in obtaining HDS active Co-W catalytic systems. Finally, no cobalt or nickel sulfide phases were detected, suggesting a wide dispersion of the promoter atoms.

Acknowledgments

We would like to acknowledge for their valuable technical assistance, Enrique Torres, Hilda Esparza, Armando Reyes, Wilberth Antunez, Daniel Lardizabal, Elizabeth González and Luz Alejandra Ponce. This work was financially supported by Conacyt and IMP, Project J31397-U and FIES-98-27-III respectively.

References

[1] H. Topsøe, B.S. Clausen and F.E. Massoth, in: *Hydrotreating Catalysis—Catalysis, Science and Technology*, Vol. 11, eds. J.R. Anderson and M. Boudard (Springer-Verlag, Berlin, 1996).
[2] E.J.M. Hensen, V.H.J. De Beer and R.A. van Santen, in *Transition Metal Sulphides, Chemistry and Catalysis, NATO ASI Series*, eds. Th. Weber, R. Prins and R.A. van Santen (Kluwer Academic Publishers, Dordrecht, 1997) p. 169.
[3] R.R. Chianelli and M. Daage, Adv. Catal. 40 (1994) 77.
[4] M. Yamada, Catal. Surv. Jpn 3 (1999) 3.
[5] D.S. Thakur and B. Delmon, J. Catal. 91 (1985) 308.
[6] G. Hagenbach, Ph. Courty and B. Delmon, J. Catal. 31 (1973) 264.
[7] R. Candia, B. Clausen and H. Topsøe, J. Catal. 77 (1982) 564.
[8] M. Zdrazil, Catal. Today 3 (1988) 269.
[9] G. Alonso, M. del Valle, J. Cruz, A. Licea-Claverie, V. Petranovskii and S. Fuentes, Catal. Lett. 52 (1998) 55.
[10] F. Pedraza and S. Fuentes, Catal. Lett. 65 (2000) 107.
[11] G. Alonso, M. Del Valle, J. Cruz, A. Licea-Claverie, V. Petranovskii and S. Fuentes, Catal. Today 43 (1998) 117.
[12] G. Alonso, V. Petranovskii, M. Del Valle, J. Cruz-Reyes, A. Licea-Claverie and S. Fuentes, Appl. Catal., A: Gen. 197 (2000) 87.
[13] R. Frety, M. Breysse, M. Lacroix and M. Vrinat, Bull. Chem. Soc. Belg. 93 (1984) 663.
[14] K. Ramanathan and S. Weller, J. Catal. 95 (1985) 249.
[15] G. Alonso, M. Del Valle, J. Cruz-Reyes and S. Fuentes, in: *Surfaces, Vacuum and their Applications, Am. Inst. Phys. Proceedings*, Vol. 378, eds. Hernandez-Calderon and R. Asomoza (Springer-Verlag, New York, 1996) p. 552.
[16] H. Nava, C. Ornelas, A. Aguilar, G. Berhault, S. Fuentes and G. Alonso, Catal. Lett. 86 (2003) 257.
[17] S. Fuentes, G. Díaz, F. Pedraza, H. Rojas and N. Rosas, J. Catal. 113 (1988) 535.
[18] K. Inamura and R. Prins, J. Catal. 147 (1994) 515.
[19] M. Sun, T. Bürgi, R. Cattaneo and R. Prins, J. Catal. 197 (2001) 172.
[20] M. Sun, M.E. Bussell, R. Prins, Appl. Catal., A 216 (2001) 103.
[21] M. Sun, P.J. Kooyman and R. Prins, J. Catal. 206 (2002) 368.
[22] V. Schwartz, M. Sun, R. Prins, J. Phys. Chem. B, 106 (2002) 2597.
[23] S.L. Soled, S. Miseo, R. Krycak, H. Vroman, T.C. Ho and K.L. Riley, U.S. Patent 6,299,760 (2001).
[24] G. Alonso, J. Yang, M.H. Siadati and R.R. Chianelli, Inorg. Chim. Acta 325 (2001) 193.
[25] G. Kishan, L. Coulier, J.A.R. van Veen and J.W. Niemantsverdriet, J. Catal. 200 (2001) 194.
[26] G. Kishan, L. Coulier, J.A.R. van Veen and J.W. Niemantsverdriet, J. Phys. Chem. B 106 (2002) 5897.
[27] M. Houalla, N.K. Nag, A.V. Sapre, D.H. Broderick and B.C. Gates, AIChE J. 24 (1978) 1015.
[28] R.R. Chianelli, Int. Rev. Phys. Chem. 2 (1982) 127.
[29] K. Pavlova, B. Panteleeva, E. Deyagina and I. Kalechits, Kinet. Katal. 6 (1965) 493.
[30] R.J.H. Voorhoeve and J.C.M. Stuiver, J. Catal. 23 (1971) 228.
[31] M. del Valle, M. Yánez, M. Avalos and S. Fuentes, in *Hydrotreating Technology for Pollution Control: Catalysts, Catalysis, and Processes, Chemical Industry Series*, Vol. 67, eds. M. Occelli and R.R. Chianelli (Marcel Dekker, New York, 1996) p. 47.
[32] J.C. Wildervanck and F. Jellinek, Z. Anorg. Allg. Chem. 328 (1964) 309.
[33] E.Z. Diemann, Z. Anorg. Allg. Chem. 432 (1977) 127.

[34] K.S. Liang, J.P. deNeufville, A.J. Jacobson and R.R. Chianelli, J. Non-Cryst. Solids 35–36 (1980) 1249.
[35] K.S. Liang, S.P. Cramer, D.C. Johnston, C.H. Chang, A.J. Jacobson, J.P. deNeufville and R.R. Chianelli, J. Non-Cryst. Solids 42 (1980) 345.
[36] R. Prada Silvy, P. Grange, F. Delannay and B. Delmon, Appl. Catal. 46 (1989) 113.
[37] P. Dufresne and F. Labruyère, US Patent 6,417,134, 2002.
[38] C. Glasson, C. Geantet, M. Lacroix, F. Labruyère and P. Dufresne, J. Catal. 212 (2002) 76.
[39] P. Afanasiev, G.F. Xia, G. Berhault, B. Jouguet and M. Lacroix, Chem. Mater. 11 (1999) 3216.
[40] G. Berhault, A. Mehta, A.C. Pavel, J. Yang, L. Rendon, M.J. Yacaman, L. Cota, A. Duarte and R.R. Chianelli, J. Catal. 198 (2001) 9.
[41] G. Berhault, L. Cota, A. Duarte, A. Mehta and R.R. Chianelli, Catal. Lett. 78 (2002) 81.
[42] L. Kao, D.R. Peacor, R.M. Coveney, G. Zhao, K.E. Dungey, M.D. Curtis and J.E. Penner-Hahn, Am. Mineral. 86 (2001) 852.
[43] J.S. Chen, Y. Wang, Y. Guo, Y.C. Zou and W. Xu, Stud. Surf. Sci. Catal. 135 (2001) 1672.
[44] N. Rueda, R. Bacaud, P. Lanteri and M. Vrinat, Appl. Catal., A: Gen. 215 (2001) 81.
[45] M. Daage and R.R. Chianelli, J. Catal. 149 (1994) 414.
[46] F. Bataille, J.L. Lemberton, P. Michaud, G. Pérot, M. Vrinat, M. Lemaire, E. Schulz, M. Breysse and S. Kasztelan, J. Catal. 191 (2000) 409.
[47] M. Breysse, G. Berhault, S. Kasztelan, M. Lacroix, F. Maugé and G. Pérot, Catal. Today 66 (2001) 15.
[48] T. Kabe, A. Ishihara and Q. Zhang, Appl. Catal., A: Gen. 97 (1993) L1.
[49] V. Meille, E. Schulz, M. Lemaire and M. Vrinat, J. Catal. 170 (1997) 29.
[50] H. Topsøe and B.S. Clausen, Appl. Catal. 25 (1986) 273.
[51] R. Candia, O. Sørensen, J. Villadsen, N-Y. Topsøe, B.S. Clausen and H. Topsøe, Bull. Soc. Chim. Belg. 93 (1984) 763.
[52] R.R. Chianelli, A.F. Ruppert, K.S. Behal, B.H. Kear, A. Wold and R. Kershaw, J. Catal. 92 (1985) 56.